Slovak University of Technology in Bratislava
Faculty of Mechanical Engineering
17th Conference on Applied Mathematics **APLIMAT 2018**

Proceedings

A MAGIC FORMULA OF NATURE

BRANDI Primo (IT), SALVADORI Anna (IT)

Abstract. The *superformula of nature*, introduced by Dutch botanist Johan Gielis to describe a wide range of shapes ([3]), is examined from the educational point of view. According to our experience, it reveals an optimal chance to propose important knowledge also in university courses of "weak" mathematics. Students become acquainted with graphic representation of functions , polar coordinates and the concept of mathematical model; moreover, they train themselves for a conscious use of parameters. It also offers the opportunity of a critical use of technology.

Keywords: elementary mathematical models, teaching innovation

Mathematics Subject Classification: Primary 97D40; Secondary 97U50, 97U70

1 Introduction

For centuries, scientists have been trying to express the forms of nature in mathematical terms; the description of the forms is one of the major problems of biology, especially when dealing with complicated shapes such as leaves or shells.
In 2003 the Dutch botanist Johan Gielis proposed a formula that can describe a wide range of natural shapes ([3]). Gielis' *superformula* represents a tool for analysis and comparison, moreover it can be used in reconstruction and recognition programs.
Despite its aspect

$$\rho = \rho(\varphi) = R(\varphi)\left(\left|\frac{1}{a}\cos\left(\frac{m}{4}\varphi\right)\right|^{p_2} + \left|\frac{1}{b}\sin\left(\frac{m}{4}\varphi\right)\right|^{p_3}\right)^{-\frac{1}{p_1}}$$

the equation reveals rather simple: it is a modified version of the equation for a circle, depending of seven parameters.
Changing one of the parameters the proportions of the shapes change, going from a perfect circle to an ellipse. By changing another one, you change the axes of symmetry, going from a circle to a triangle, a square, a pentagon, and so on. By changing both the proportions and the symmetry, shapes are produced with any number of smooth or irregular sides.
You can also produce non-biological forms, such as snowflakes or crystals.
Of course also a three-dimensional version of the formula hold, with many interesting applications.

In our contribution we wish to focalize a different aspect: the potentiality of the formula for educational purposes. Students, fascinated by the wonderful shapes, let themselves be led into the mathematical world where they acquire a wide range of knowledge without difficulty and become aware of the important unifying properties of the discipline.
For didactical purpose we have chosen to present superformula step by step as subsequent changes to the equation of a circumference. In this way, introducing one parameter at a time, we have the opportunity to show clearly the role played by each parameter.
More precisely the paper is organized as follows.

Section 2. From circumference to super-circumferences (parameter p).

Section 3. From super-circumferences to super-ellipses (parameters a and b).

Section 4. From Cartesian to polar coordinates (parameters r and φ).

Section 5. Three different exponential parameters $p_1\ p_2\ p_3$ take the place of p.

Section 6. The argument φ is revised as phase parameter $\frac{m}{4}\varphi$.

Section 8. Scale parameter r is replaced by a function $R(\varphi)$.

Sections 7 and 9 are devoted to applications of superformula to natural shapes. See also Section 3.3, 8.1 and 8.2 for other examples.

The graphics in the present paper were implemented by the Authors with Mathematica ver.7.

2 The *squared* circle

For a long time the circle and the square have been considered as "opposed" figures, basic models with completely different peculiarities. At the beginning of the nineteenth century French mathematician Gabriel Lamé (Tours 1795 – Paris 1870) revolutionized this view by proving that circles and squares could be represented by a single equation.
As it is well known, the equation of the circumference with center in the origin and radius r is the following

$$x^2 + y^2 = r^2 \tag{1}$$

Lamé introduced the following generalization of the circumference equation

$$|x|^p + |y|^p = r^p \qquad \text{with} \qquad p > 0 \tag{1'}$$

which today is known as **Lamé circumference**. The introduction of parameter p allows to extend widely the shapes that can be represented by the equation, as we will show in the next section.

2.1 The role of parameter *p*

Of course, for $p = 2$ we get usual circumference equation, but as the parameter $p \in R^+$ varies, other interesting figures are described, as the following images show

Lamé super circumferences

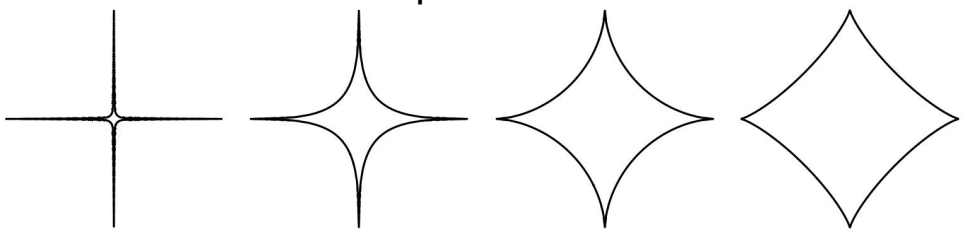

Fig. 1. p = 0.2 Fig. 2. p = 0.4 Fig. 3. p = 0.6 Fig. 4. p = 0.8

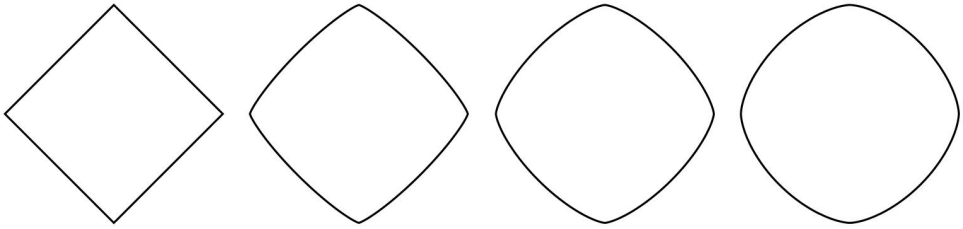

Fig. 5. p = 1 Fig. 6. p = 1.2 Fig. 7. p = 1.6 Fig. 8. p = 2

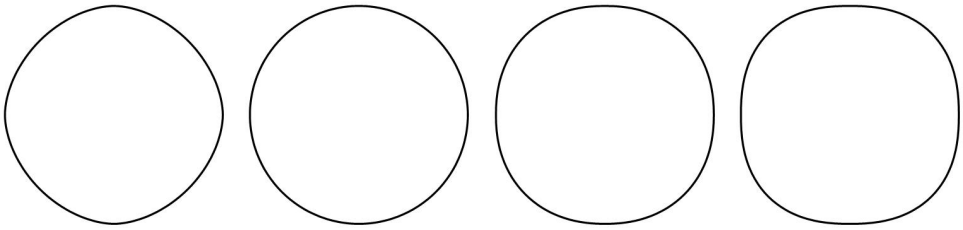

Fig. 9. p = 2.4 Fig. 10. p = 3 Fig. 11. p = 6 Fig. 12. p = 10

For very small values of the parameter $(p \cong 0)$ C_p is constituted by two orthogonal segments of length 2 which intersect in the origin; as the values of p increases, we get "asteroid" figures which gradually evolve first to the rhombus C_1, then to the circumference C_2 and finally, for great values of the parameter C_p they are getting closer to the square with the sides parallel to the axes $[-1,1]^2$.

3 Super-ellipses

Ellipse can be considered as a generalization of the circumference

$$(x/a)^2 + (y/b)^2 = 1 \tag{2}$$

where $a > 0$ and $b > 0$ are the length of the axes. If $a = b$ it reduces to a circumference.
Thus Lamé proposed also the equations of super-ellipses

$$|x/a|^p + |y/b|^p = 1 \quad p > 0 \tag{2'}$$

which depends on three parameters a, b, p.
The contribution of each parameter can be easily deduced from the previous remark.

3.1 Super-ellipses in the real world

For more than one century, Lamé equation did not appear to be of great interest until it was re-discovered by Dutch architect Piet Hein and has founded a major role in architecture and design. We wish to recall just a meaningful example.

In 1959, the city of Stockholm was facing a building design problem whose brilliant solution would have provided an innovative idea from which many designers have drawn inspiration. In Sergel's Torg two large north-south and east-west traffic arteries intersected, creating a vast rectangular space (about 200 yards long) that was intended for commercial use. The designers faced a problem that was more difficult than expected: the shape of the building.

A rectangular construction would optimize the available space for the shopping but the corners would interfere with the surrounding traffic fluidity. An ellipsoidal design would have sacrificed space for business, it would not be harmonized with the rectangular surface of the available space and would not have solved the traffic difficulties of cars satisfactorily.

Hein choose a shape that could satisfied all the requests: the super-ellipse with $a/b = 6/5$ and $p = 5/2$ (see Fig. 13 and 14).

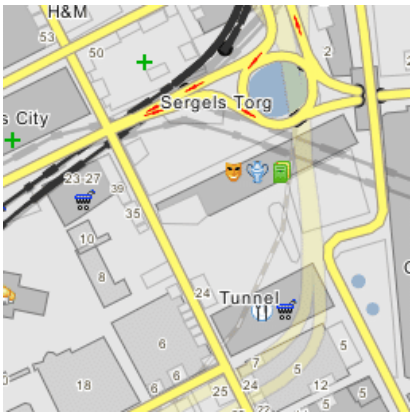

Fig. 13. Map of Stockholm.

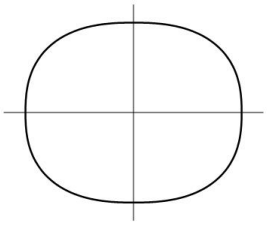

$a/b = 6/5$
$p = 5/2$

Fig. 14. super-ellipse.

Fig. 15. Sergel's Torg.

After the brilliant solution proposed by Hein, super-ellipses often met the favor of designers and architects in Canada, France, Japan, the United States and Mexico.

Piet Hein's collaboration with Bruno Mathsson, a famous Swedish designer, produced several super-elliptical artifacts: glasses, plates, desk lamps (very popular in the sixties), chairs and beds. (see http://www.piethein.dk/)

An interesting link between super-ellipses and nature are the sections of bamboo plants. Some species of bamboo cane have *square* sections at the bottom (Chimono bambusa quadrangularis), more precisely the sections have the form of super-circumferences. These square bamboos are more resistant than circular ones and are widely used for buildings in the east countries.

Fig. 16 Chimono bambusa quadrangularis [2] .

4 The first step toward super-formula

In 2003 ([2],[3]) Dutch biologist Johan Gielis gave new life to Lamé equation by introducing some modifications that produced a very ductile formula. As we will show in the following, Gielis equation is able to generate a multiplicity of forms of plants and living beings.

4.1 From Cartesian to Polar coordinates.

If we pass to polar coordinates $\begin{cases} x = \rho\cos\varphi \\ y = \rho\sin\varphi \end{cases}$ super-ellipses equation becomes

$$\rho = \rho(\varphi) = r\left(\left|\frac{1}{a}\cos\varphi\right|^p + \left|\frac{1}{b}\sin\varphi\right|^p\right)^{-\frac{1}{p}} \tag{3}$$

This formula adds two more parameters to super ellipses. Let us show the contribution of each parameter on the shape of the corresponding figure.

4.2 The role of parameter *r*

Of course r is a *scale* parameters that controls figure dimension. The following image shows a family of super-ellipses corresponding to different values of the parameter r (from 1 to 5).

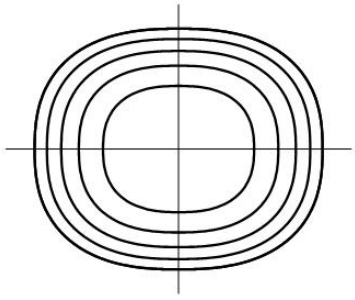

Fig. 17. Super-ellipses.

4.3 The role of parameter φ

We can consider the particular case $a = b = r = 1$

Observe that function $\rho = \rho(\varphi)$ $\varphi \in [0, 2\pi]$ represent the length of the vector ray corresponding to angle φ.

For this reason, the local minima and maxima of ρ play a fundamental for the figure shape. Since that function ρ is the reciprocal of function

(3') $$f_p(\varphi) = \left(|\cos\varphi|^p + |\sin\varphi|^p\right)^{\frac{1}{p}} \quad \varphi \in [0, 2\pi].$$

the local maximum and minimum points of ρ correspond to the local minimum and maximum points of f; in fact we have

$$\rho(\varphi_0) \le \rho(\varphi) \quad \forall \varphi \in I(\varphi_0) \quad \Leftrightarrow \quad f_p(\varphi_0) \ge f_p(\varphi) \quad \forall \varphi \in I(\varphi_0).$$

4.4 Again on the role of parameter *p*

As the parameter p varies, $\rho_p(\varphi) = \left(|\cos\varphi|^p + |\sin\varphi|^p\right)^{-\frac{1}{p}}$ assume different shapes, corresponding to the different values of the maxima e minima of function

$$f_p(\varphi) = \left(|\cos\varphi|^p + |\sin\varphi|^p\right)^{\frac{1}{p}} \quad \varphi \in [0, 2\pi].$$

For $p = 1$ (Manhattan metric) it can easily proved that function

$$f_1(\varphi) = |\cos\varphi| + |\sin\varphi| \quad \varphi \in [0, 2\pi]$$

admits

$$\min f_1 = 1 \qquad \max f_1 = \sqrt{2}$$

and presents: 4 minimum points $\varphi_j = j\frac{\pi}{2}$; 4 maximum points $\varphi_j = (2j+1)\frac{\pi}{4}$ $j = 0,1,2,3$.

The following images shows as the shape of f_1 is transmitted to that of ρ_1 .

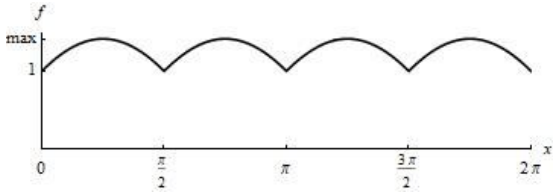

Fig. 18. Function f_1 $\max f_1 = \sqrt{2}$.

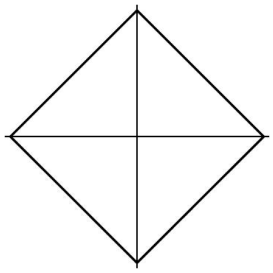

Fig. 18'. Function ρ_1.

It is easy to prove that functions $f_p(\varphi)$ still admits 4 minimum points and 4 maximum points for every value of parameter p .

For $0 < p < 2$ they are the same of f_1, while for $p > 2$ they are inverted

minimum points: $\varphi_j = (2j+1)\frac{\pi}{4}$ maximum points $\varphi_j = j\frac{\pi}{2}$ $j = 0,1,2,3$.

Let us summarize the results in the following table.

parameter	min f_p	max f_p	
$0 < p < 1$	1	It progressively decreases as p increases	
$p = 1$	1	$\sqrt{2}$	(Manhattan metric)
$1 < p < 2$	1	It progressively decreases as p increases	
$p = 2$	1	1 (constant function)	(Euclidean metric)
$p > 2$	It progressively decreases as p increases	1	

The following images illustrate the results of the table.

The role of parameter p

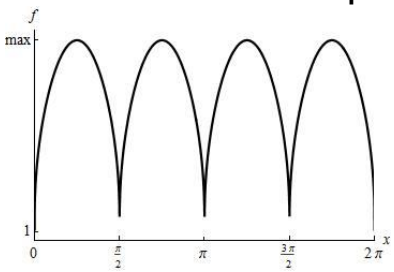

Fig. 19. $p = 0.1$ max $f \cong 22.62$ min $f = 1$

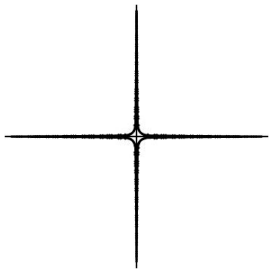

Fig. 19'.

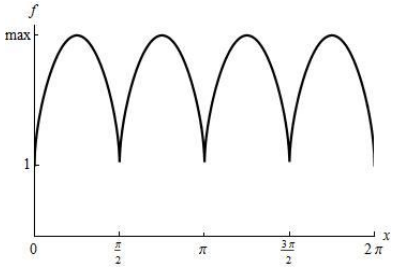

Fig. 20. $p = 0.5$ max $f \cong 2.82$ min $f = 1$

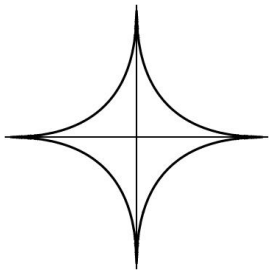

Fig. 20'.

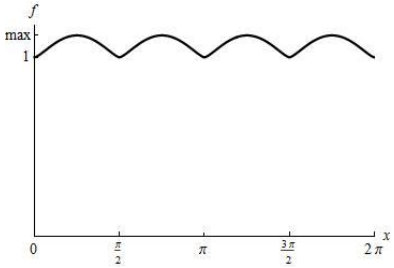

Fig. 21. $p = 1.5$ max $f \cong 1.12$ min $f = 1$

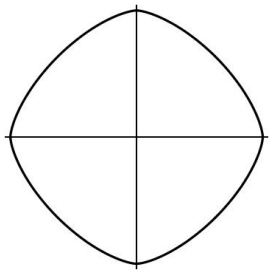

Fig. 21'.

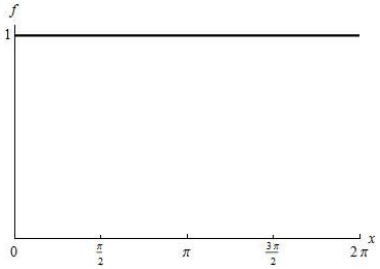

Fig. 22. $p = 2$ max $f = \min f = 1$

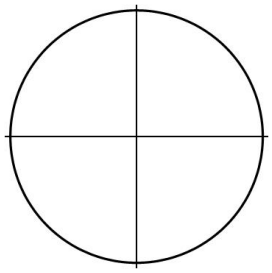

Fig. 22'.

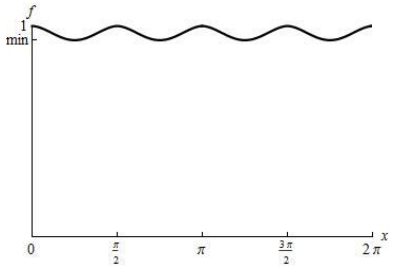

Fig. 23. $p = 2.5$ max $f = 1$ min $f \cong 0.93$

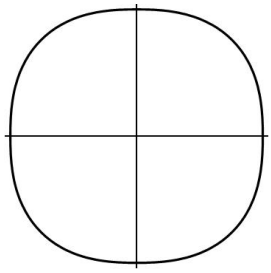

Fig. 23'.

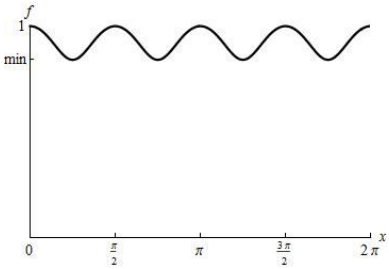

Fig. 24. $p = 4$ max $f = 1$ min $f \cong 0.84$

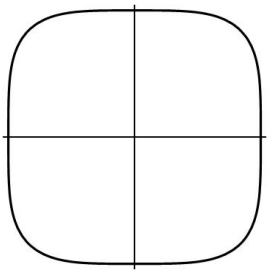

Fig. 24'.

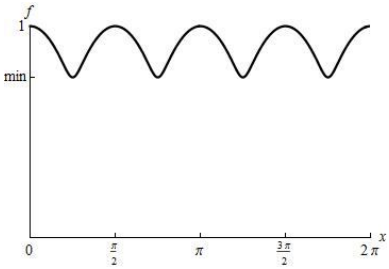

Fig. 25. $p = 10$ max $f = 1$ min $f \cong 0.75$

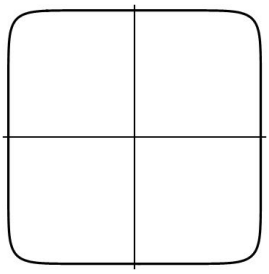

Fig. 25'.

5 A second first step toward super-formula

A further extension of super-ellipses equation proposed by Gielis consists on adopting three different values for the exponents $p_i \quad i = 1, 2, 3$

$$\rho = r\left(\left|\frac{1}{a}\cos\varphi\right|^{p_2} + \left|\frac{1}{b}\sin\varphi\right|^{p_3}\right)^{-\frac{1}{p_1}} \tag{4}$$

Let us show the strategic power of this innovation.

5.1 The role of parameters p_1, p_2, p_3

We can consider again the particular case $a = b = r = 1$.
First of all, note that parameter p_2 acts on the horizontal component, while parameter p_3 on the vertical component.
More precisely, each parameter produces the effect of a non-linear transformation, respectively

$$\begin{cases} x' = x^{p_2} \\ y' = y \end{cases} \qquad \begin{cases} x' = x \\ y' = y^{p_3} \end{cases}$$

Let us assume $p_1 = 1$ and show the role of parameters p_2 and p_3 by means of some images.

The role of parameter p_2 (p_1=p_3=1, m=4)

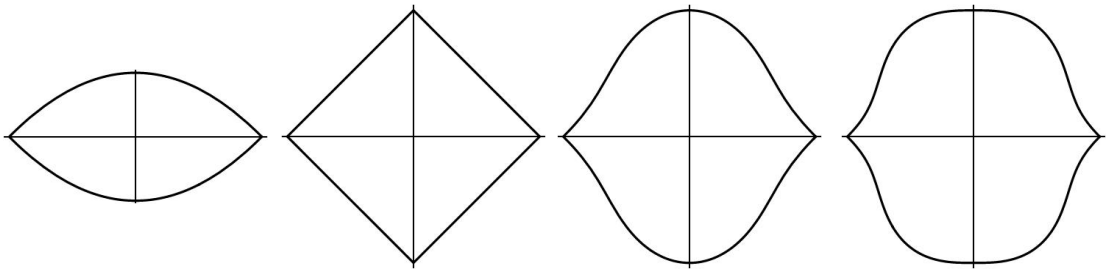

Fig. 26. $p_2 = 0$ Fig. 27. $p_2 = 1$ Fig. 28. $p_2 = 2$ Fig. 29. $p_2 = 3$

The role of parameter p_3 (p_1=p_2=1, m=4)

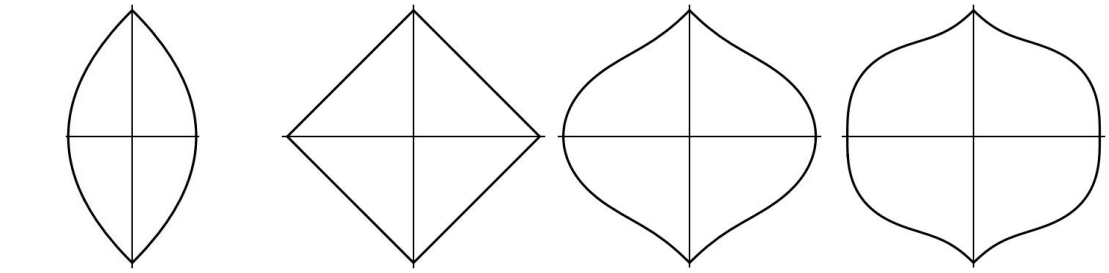

Fig. 30. $p_3 = 0$ Fig. 31. $p_3 = 1$ Fig. 32. $p_3 = 2$ Fig. 33. $p_3 = 3$

Note that parameter p_1 produces an effect of multidirectional deformation.
Let us see some examples, assuming $p_2 = p_3 = 1$.

The role of parameter p_1 (p_2=p_3=1, m=4)

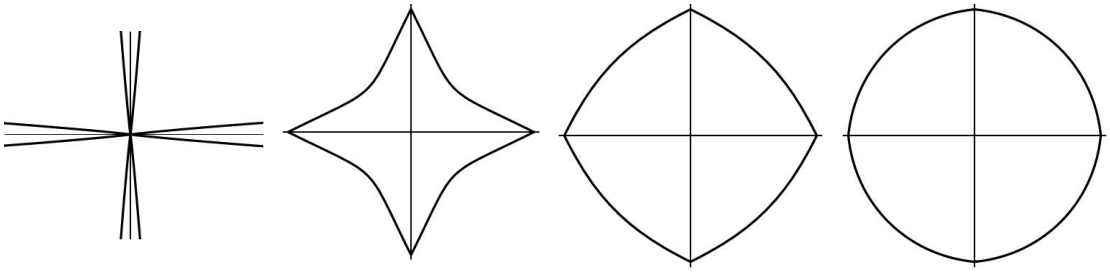

Fig. 34. $p_1 = 0.01$ Fig. 35. $p_1 = 0.5$ Fig. 36. $p_1 = 2$ Fig. 37. $p_1 = 10$

6 A third step: the introduction of phase parameter

Gielis observes that all the figures above have the disadvantage of a limited symmetry, as it happen with super-ellipses. Precisely they have a rotational symmetry of order four, while in nature there are organisms with hexagonal or pentagonal symmetry.
For this reason he adds a *phase parameter* k :

$$\rho(\varphi) = r\left(\left|\frac{1}{a}\cos(k\varphi)\right|^{p_2} + \left|\frac{1}{b}\sin(k\varphi)\right|^{p_3}\right)^{-\frac{1}{p_1}} \qquad (5)$$

To show the role of phase parameter, we can consider the particular case $a = b = r = 1$ $p_1 = p_2 = p_3 = 1$

$$\rho_k(\varphi) = \left(\left|\cos(k\varphi)\right| + \left|\sin(k\varphi)\right|\right)^{-1}$$

Note that function

$$f_k(\varphi) = \left|\cos(k\varphi)\right| + \left|\sin(k\varphi)\right| \quad \varphi \in [0, 2\pi] \tag{5'}$$

admits the same maxima and minima of functions f_1 in Section 4.4 (see Fig. 18), but the number of maximum and minimum points is now 4k. They are respectively

$$\text{minimum points: } \varphi_j = \frac{j}{k}\frac{\pi}{2} \quad j = 0,1,\ldots,4k-1$$

$$\text{maximum points} \quad \varphi_j = \frac{2j+1}{k}\frac{\pi}{4} \quad j = 0,1,\ldots,4k-1.$$

The role of parameter k

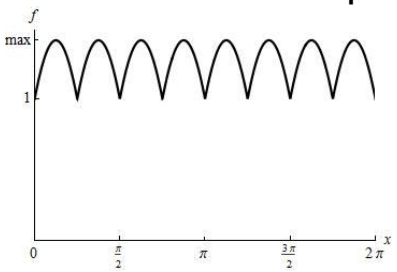

Fig. 38. $k = 2$ $\max f = \sqrt{2}$ $\min f = 1$

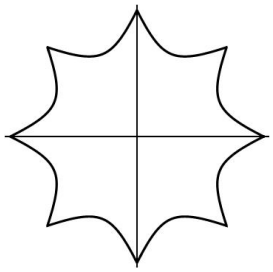

Fig. 38'.

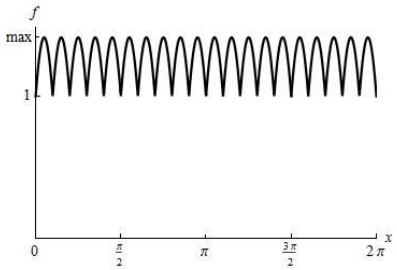

Fig. 39. $k = 5$ $\max f = \sqrt{2}$ $\min f = 1$

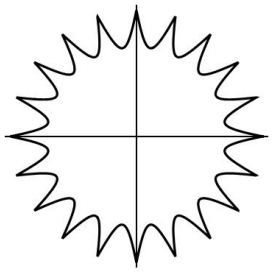

Fig. 39'.

For this reason Gielis proposed to chose as phase parameter the number

$$k = \frac{m}{4}.$$

Thus the equation becomes

$$\rho = \rho(\varphi) = r\left(\left|\frac{1}{a}\cos\left(\frac{m}{4}\varphi\right)\right|^{p_2} + \left|\frac{1}{b}\sin\left(\frac{m}{4}\varphi\right)\right|^{p_3}\right)^{-\frac{1}{p_1}} \tag{6}$$

6.1 The role of parameter *m*

Let us discuss the fundamental role played by phase parameter m, assuming $a = b = r = 1$, $p_1 = p_2 = p_3 = 1$.

We start form the case of integer values for parameter *m* (see Fig. 40-48)

***m* integer**

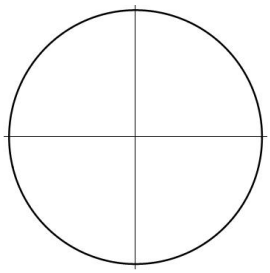

Fig. 40. $m = 0$

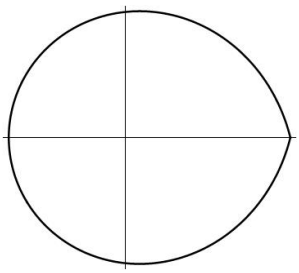

Fig. 41. $m = 1$

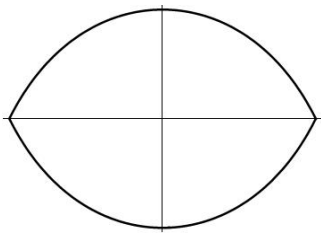

Fig. 42. $m = 2$

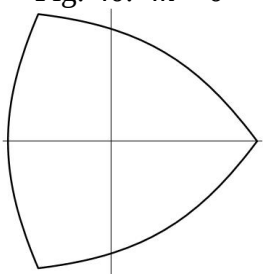

Fig. 43. $m = 3$

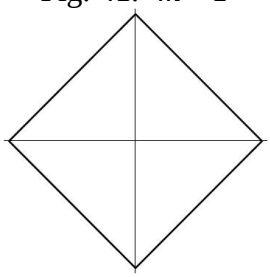

Fig. 44. $m = 4$

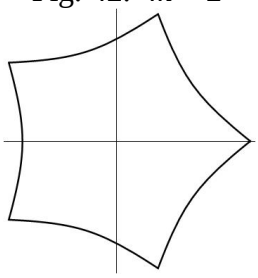

Fig. 45. $m = 5$

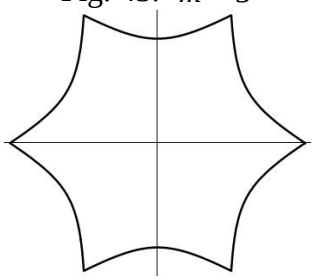

Fig. 46. $m = 6$

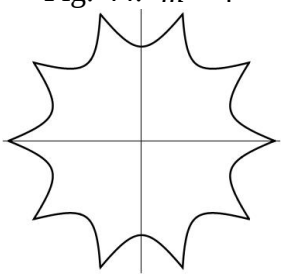

Fig. 47. $m = 10$

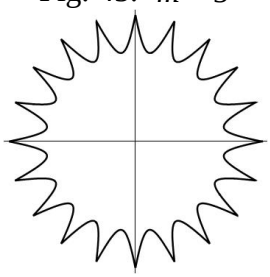

Fig. 48. $m = 20$

For Lamè super-ellipses the plane is ideally divided into four parts (the four quadrants) and all the figures have the same four fixed points on the circle.

Now the plane can be divided into *m* sectors. As we can see from the previous images, the phase parameter allows the sides to bend in and out like a fan. Moreover *m* determines the number of fixed points on the unit circle and the space between them. In other words *m* represents the number of rotational symmetries.

Assume now that $m = \mu/\upsilon$ is a rational number. The figure will close after υ rotations, while μ determines the number of angles. In particular, if *m* is integer, after a rotation the figure closes and in the subsequent rotations the figure remains unchanged (see Fig. 40-54).

***m* rational**

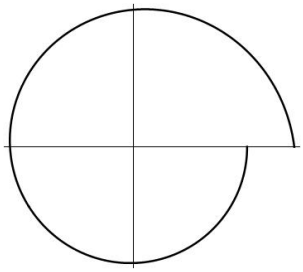

Fig. 49. $m = 1/2$
$0 \le \varphi \le 2\pi$

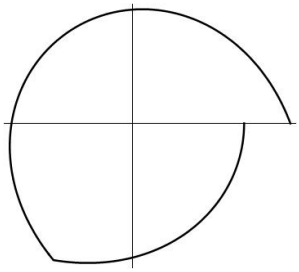

Fig. 50. $m = 3/2$
$0 \le \varphi \le 2\pi$

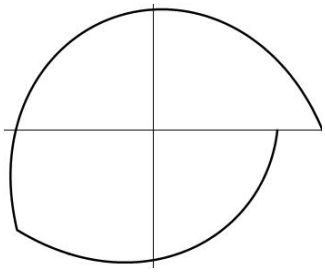

Fig. 51. $m = 5/3$
$0 \le \varphi \le 2\pi$

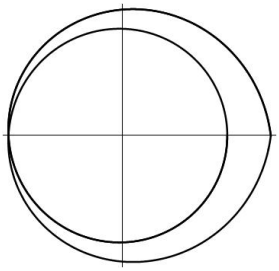

Fig. 52. $m = 1/2$
$0 \le \varphi \le 2 \cdot 2\pi$

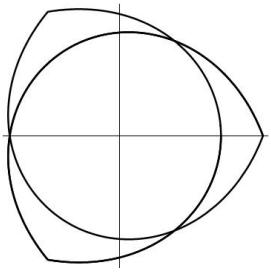

Fig. 53. $m = 3/2$
$0 \le \varphi \le 2 \cdot 2\pi$

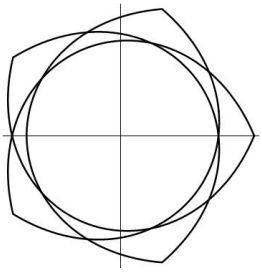

Fig. 54. $m = 5/3$
$0 \le \varphi \le 2 \cdot 3\pi$

While if *m* is not rational, the figure generated after a single rotation does not close, as the following examples show (see Fig. 55-57).

***m* not rational**

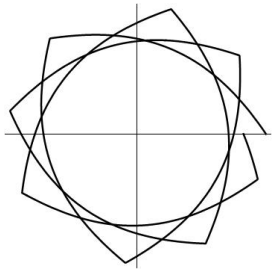

Fig. 55. $m = e$
$0 \le \varphi \le 6\pi$

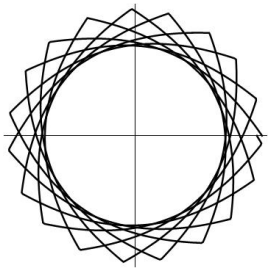

Fig. 56. $m = e$
$0 \le \varphi \le 14\pi$

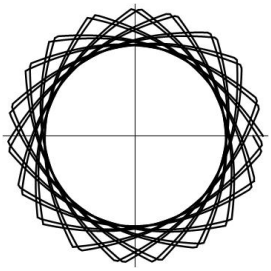

Fig. 57. $m = e$
$0 \le \varphi \le 28\pi$

Of course the number of possible shapes increase greatly if we assume different values for the exponent p.

In the particular case $m = 1$, we have a circle for $p = 2$, but for every $p \neq 2$ the figures present an angular points (see Fig. 58, 59). Precisely, for $0 < p < 2$ the angular points is on the right, while for $p > 2$ it is on the left (rotated by π).

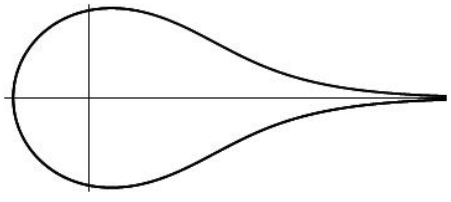

Fig. 58. $m = 1 \quad p = 0.3$

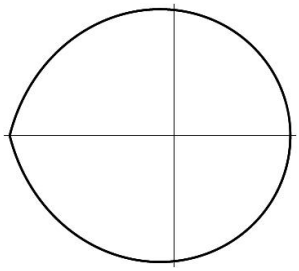

Fig. 59. $m = 1 \quad p = 5.000$

In the particular case $m = 2$ figures similar to the previous case are obtained, but with two angular points instead of one.

7 Some examples: nature's forms and polygons

The following images show the great potential offered by the variability of the parameters

The role of parameter p_1 (p_2=p_3=1, m=4)

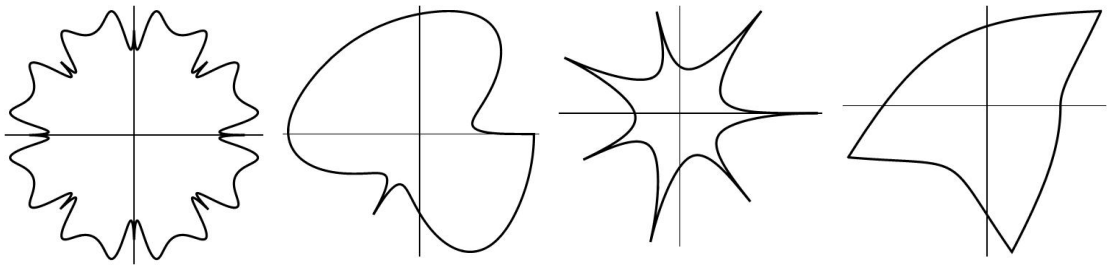

Fig. 60. $m = 16 \;\; p_1 = 1 \;\; p_2 = 10 \;\; p_3 = 0.3$

Fig. 61. $m = 3 \;\; p_1 = 0.5 \;\; p_2 = 10 \;\; p_3 = 0.3$

Fig. 62. $m = 7 \;\; p_1 = 0.5 \;\; p_2 = 0.5 \;\; p_3 = 0.3$

Fig. 63. $m = 3 \;\; p_1 = 10000 \;\; p_2 = p_3 = 2018$

As we have already observed, by means of formula (6) we can describe the circles, ellipses and rectangles. Note that we can also represent all the regular polygons together with their concave and convex versions (i.e. sub-polygons and super-polygons), as the following images show.

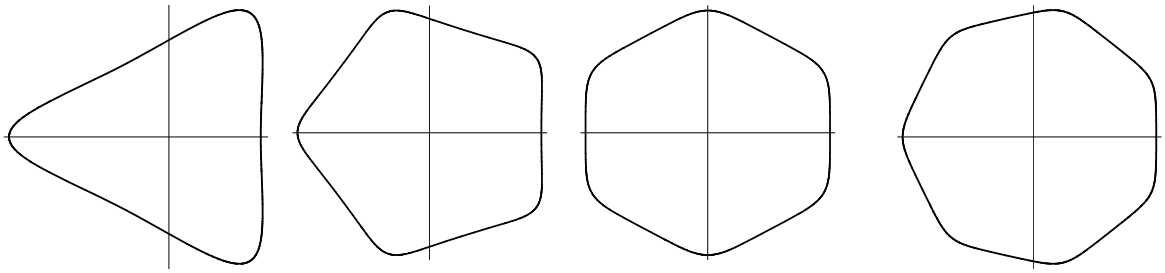

Fig. 64. $m = 3 \;\; p_1 = 5 \;\; p_2 = p_3 = 10$

Fig. 65. $m = 5 \;\; p_1 = 6.5 \;\; p_2 = p_3 = 4.65$

Fig. 66. $m = 6 \;\; p_1 = 10.65 \;\; p_2 = p_3 = 4.65$

Fig. 67. $m = 7 \;\; p_1 = 15 \;\; p_2 = p_3 = 4.65$

8 Superformula

The final Gielis' generalization of equation (6) consists on replacing parameter r with a function of the variable φ

$$\rho = \rho(\varphi) = R(\varphi)\left(\left|\frac{1}{a}\cos\left(\frac{m}{4}\varphi\right)\right|^{p_2} + \left|\frac{1}{b}\sin\left(\frac{m}{4}\varphi\right)\right|^{p_3}\right)^{-\frac{1}{p_1}} \qquad (8)$$

Of course, this innovation improves the performance . Let us discuss two remarkable particular cases.

8.1 Spirals

Let us consider the particular case of the function

$$R(\varphi) = \varphi$$

which is constant in each period, but whose argument increases with increasing periods. Inserted in the superformula it leads to the representation of spirals, as the following examples show.

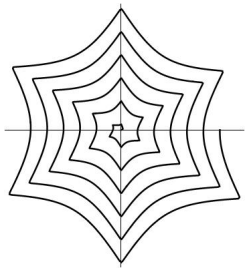

Fig. 68.
$m = 6\ p_1 = p_2 = p_3 = 100$
$0 \le \varphi \le 12\pi$

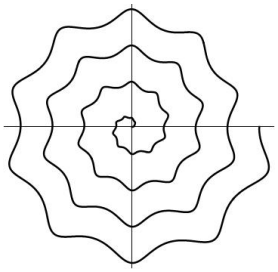

Fig. 69.
$m = 10 \quad p_2 = p_3 = 5$
$p_1 = 8 \quad 0 \le \varphi \le 8\pi$

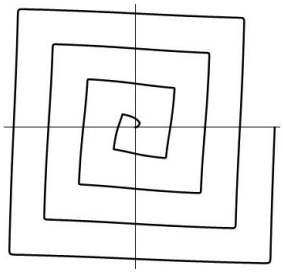

Fig. 70.
$m = 4\ p_1 = p_2 = p_3 = 100$
$0 \le \varphi \le 8\pi$

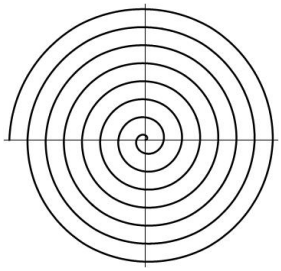

Fig. 71.
$m = 6 \quad p_2 = p_3 = 1$
$p_1 = 100 \quad 0 \le \varphi \le 15\pi$

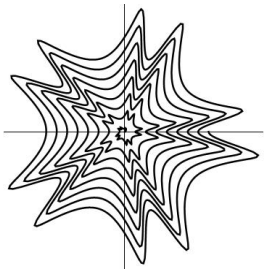

Fig. 72.
$m = 10 \quad p_2 = 50\ p_3 = 5$
$p_1 = 8 \quad 0 \le \varphi \le 16\pi$

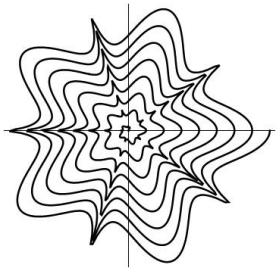

Fig. 73.
$m = 10 \ \ p_2 = 0{,}5 \ \ p_3 = 2$
$p_1 = 1 \quad 0 \le \varphi \le 16\pi$

8.2 Flowers

Function $$R(\varphi) = \left|\cos\frac{m}{2}\varphi\right|$$

admits $\max R(\varphi) = 1$, $\min R(\varphi) = 0$ and presents m maximum points and m minimum ones. Inserted in the superformula it allows to represent flower petals, as the following examples show.

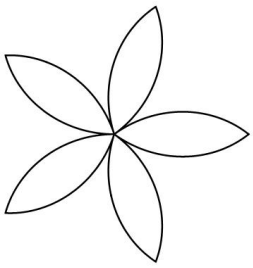

Fig. 74. $m = 5$
$p_1 = p_2 = p_3 = 1$

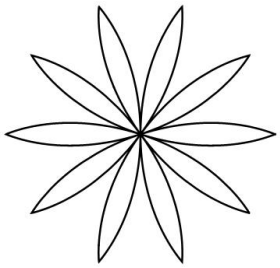

Fig. 75. $m = 10$
$p_1 = p_2 = p_3 = 1$

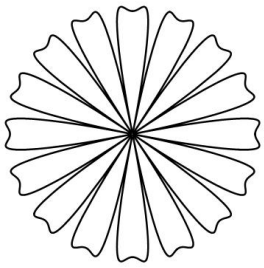

Fig. 76. $m = 16$
$p_1 = 1 \ \ p_2 = p_3 = 5$

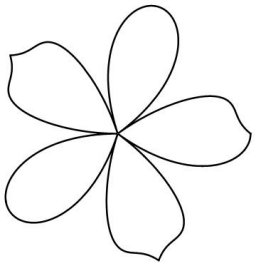

Fig. 77. $m = 5$
$p_3 = p_1 = 1 \quad p_2 = 10$

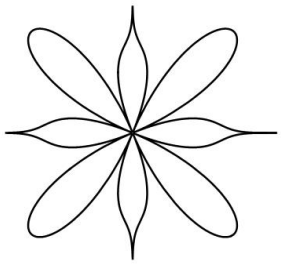

Fig. 78. $m = 8$
$p_2 = 5 \quad p_3 = 0.3 \quad p_1 = 1$

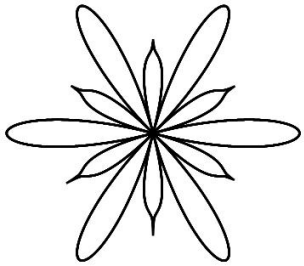

Fig. 79. $m = 12$
$p_2 = 0.1 \quad p_3 = 5 \quad p_1 = 1$

The previous figures show that a different values of the parameters p_2 and p_3 produces asymmetries between the petals. Parameter p_1 adjusts the roundness, as the following sequences of images shows (where $m = 5 \quad p_2 = p_3 = 1$).

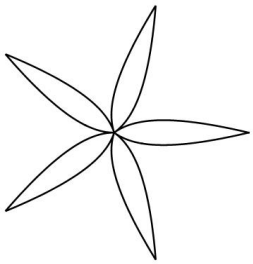

Fig. 80. $p_1 = 0.3$

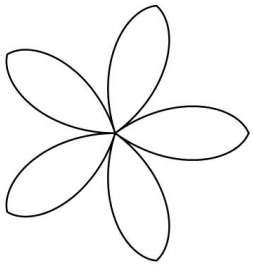

Fig. 81. $p_1 = 3$

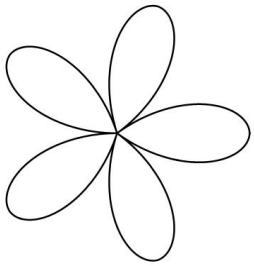

Fig. 82. $p_1 = 30$

9 A selected list of examles

Let's now propose some examples, taken from ([1]), that testify superformula potentiality on a faithful reproduction of various forms of nature.

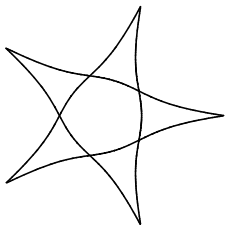

$a = b = 10 \quad m = 5$
$p_1 = p_3 = 2 \quad p_2 = 1$
$0 \le \varphi \le 2 \cdot 2\pi$

Fig. 83. Calys and sepals of roses.

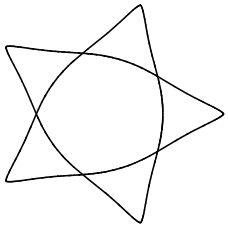

$a = b = 10 \quad m = 5$
$p_1 = 3.6 \; p_3 = 2.5 \; p_2 = 1.4$
$0 \le \varphi \le 2\pi$

Fig. 84. Succulent flowers.

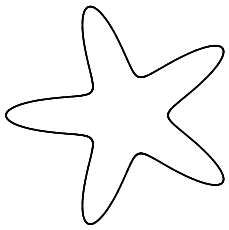

$$a = b = 10 \quad m = 5$$
$$p_2 = p_3 = 5 \quad p_1 = 1$$
$$0 \le \varphi \le 2 \cdot 2\pi$$

Fig. 85. Starfish.

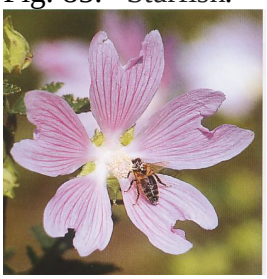

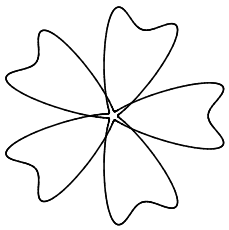

$$a = b = 10 \quad m = 5$$
$$p_1 = 1 \; p_3 = 5.9 \; p_2 = 4.6$$
$$0 \le \varphi \le 2 \cdot 2\pi$$

Fig. 86. Flower.

$$a = b = 1 \quad m = 10$$
$$p_2 = p_3 = 5 \quad p_1 = 8$$
$$0 \le \varphi \le 14 \cdot 2\pi$$
$$R(\varphi) = \varphi^{2.55}$$

Fig. 87. Pleuroploca trapezium.

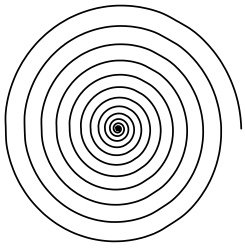

$$a = b = 1 \quad m = 6$$
$$p_2 = 0 \quad p_3 = p_1 = 100$$
$$0 \le \varphi \le 14 \cdot 2\pi$$
$$R(\varphi) = \varphi^{2.4}$$

Fig. 88. Architectonica perspectiva.

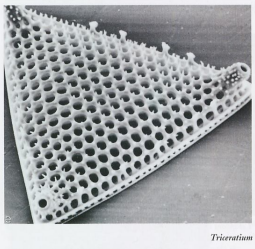

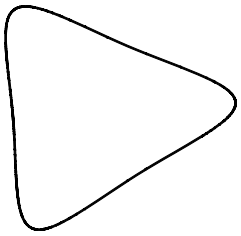

$$a = b = 10 \quad m = 3$$
$$p_1 = 5 \; p_3 = p_2 = 10$$
$$(11/36) \cdot 2\pi \le \varphi \le (11/36) \cdot 2\pi + 2\pi$$

Fig. 89. Diatomee.

References

[1] BRACCI, P., *La superformula della natura*, Tesi di laurea in Matematica, Università di . Perugia (2013/14)
[2] GIELS, J., A *generic geometric transformation that unifies a wide range of natural and abstract shapes*, American Journal of Botany, 90, 333-338, 2003
[3] GIELS, J., *Inventing the circle: the geometry of nature*, Geniaal, 2003
[4] URL, http://www.genicap.com/

Current address

Brandi Primo
Department of Mathematics and Informatics
University of Perugia
via Vanvitelli 1, 06123 Perugia, Italy
E-mail: primo.brandi@unipg.it

Salvadori Anna
Department of Mathematics and Informatics
University of Perugia
via Vanvitelli 1, 06123 Perugia, Italy
E-mail: anna.salvadori@unipg.it